

Prospective Study

Prone Position MRI of the Lumbar Spine in Patients With Low Back Pain and/or Radiculopathy Refractory to Treatment

Martin Avellanal, MD, PhD¹, Antonio Ferreiro, MD, PhD², Irene Riquelme, MD¹, André P. Boezaart MD, PhD^{3,4,5}, Alberto Prats-Galino, MD, PhD⁶, and Miguel A. Reina, MD, PhD^{3,7,8}

From: ¹The Pain Clinic, University Hospital Sanitas La Moraleja, Madrid, Spain; ²Department of Radiology, Madrid University Hospital, Madrid, Spain; ³The Division of Acute and Perioperative Pain Medicine, Department of Anesthesiology, University of Florida College of Medicine, Gainesville, Florida, USA; ⁴The Alon P. Winnie Research Institute, Still Bay, Western Province, South Africa; ⁵The Lumina Pain Medicine Collaborative, Surrey, United Kingdom; ⁶Laboratory of Surgical Neuro Anatomy, Human Anatomy and Embryology Unit, Faculty of Medicine, Universitat de Barcelona, Barcelona, Spain; ⁷The CEU-San Pablo University School of Medicine, Madrid, Spain; ⁸The Department of Anesthesiology, Madrid-Montepíncipe University Hospital, Madrid, Spain

Address Correspondence: Martin Avellanal, MD, PhD
The Pain Clinic, University Hospital Sanitas La Moraleja
Av. Francisco Pi y Margall, 81,
28050, Madrid, Spain
E-mail: avellanalmartin@gmail.com

Disclaimer: There was no external funding in the preparation of this manuscript.

Conflict of interest: Each author certifies that he or she, or a member of his or her immediate family, has no commercial association (i.e., consultancies, stock ownership, equity interest, patent/licensing arrangements, etc.) that might pose a conflict of interest in connection with the submitted manuscript.

Background: There are patients with limiting low back pain (LBP) with or without radicular pain in whom conventional supine magnetic resonance imaging (MRI) show no causative pathology. Despite the limitations of dynamic axially loaded MRI examinations, these imaging studies have shown a striking ability to diagnose pathology unrecognized by conventional MRI. The difference in findings between supine and prone MRI with patient symptom correlation has not been studied.

Methods: Nineteen patients suffering from chronic moderate-to-severe LBP and/or radicular pain nonresponsive to conventional therapy or interventional treatment, were included in this study. Both supine and prone MRIs were performed and analyzed by a neuroradiologist. Specific supine and prone measurements were registered, including spinal canal area, lateral recess diameter, foraminal area, and ligamentum flavum thickness. Three-dimensional MRI reconstructions of varying pathology patterns were created.

Results: The mean patient age was 48.7 years (range [R]: 30-69), 63% of patients were women. The mean numeric pain score was 6.5 (R: 4-8). In 52.6% of cases, disc pathology/increased disc pathology was seen only on prone imaging. We observed significant buckling and increased thickness of the ligamentum flavum in 52.6 % of cases in the prone position that was absent from the supine MRIs. We also documented varying grades of spondylolisthesis and facet joint subluxation resulting in significant foraminal stenosis in 26.3% of prone cases not seen from supine MRIs.

Conclusions: Four patterns of pathological findings have been identified by MRI performed in the prone position. These findings were not observed in the supine position. Prone MRI can be a significant and useful tool in the diagnosis and treatment of patients with back pain refractory to treatment whose conventional supine MRIs appeared unremarkable.

Key words: Low back pain, magnetic resonance imaging, spinal instability, positional MRI, prone MRI

IRB approval was obtained from the Hospital Group Madrid Clinical Research Ethics Committee (Code: 17.01.1040-GHM).

Pain Physician 2022: 25:409-418

Manuscript received: 11-09-2021
Revised manuscript received: 01-23-2022
Accepted for publication: 03-23-2022

Free full manuscript:
www.painphysicianjournal.com

In clinical practice, it is not unusual to encounter patients with moderate-to-severe chronic low back pain (LBP) and/or radicular pain presenting with unremarkable conventional magnetic resonance imaging (MRI) findings. Such patients are commonly scheduled for an interlaminar or transforaminal epidural block performed in the prone position. While prone, the patient's usual pain is commonly elicited suggesting some degree of stenosis (2). However, limited improvement in these patients lasting only a few days or early relapse suggests, among other causes, mechanical instability.

In reviewing the clinical condition of such patients, we observed that most of these patients did not report pain while in the supine position. Some patients even experienced pain improvement while supine. These same patients did report pain while standing or sitting. We typically did not ask them how they tolerated the prone position.

Segmental lumbar motion is commonly evaluated using dynamic upright flexion and extension radiographic images. Segmental instability is defined by comparative vertebral body subluxation > 3 mm or sagittal angulation of >15° to 25° (1). X-rays, however, are insensitive to the degree of soft tissue involvement.

Dynamic upright MRI in standing, in flexion, or in the seated position has been performed with authors describing loading changes (2-4). However, these studies were performed with low-field-strength open MRIs with limited diagnostic accuracy.

There are isolated prone MRI studies that have been used to diagnose anchored medulla (5), and adhesive arachnoiditis (6), and to study the real proximity of the great vessels (aorta, vena cava, and iliac arteries) to the vertebral bodies in the same prone position in which surgical arthrodesis is performed (7). There are also studies using prone computed tomography (CT) (e.g., for the study of idiopathic scoliosis in adolescents) (8). One supine MRI study was performed using a lumbar pillow. The authors argued that they found similar results to those of a standing MRI for the detection of spinal canal stenosis. However, the results are inconsistently reproducible, and the type of lumbar pillow that should be used is debatable (9).

Prone MRI of the lumbar spine does not require special imaging equipment, although it is necessary to make modifications in the technique. Therefore, we proposed a comparative MRI study with patients being imaged in both the supine and prone positions. We concentrated on patients with equivocal or unremarkable conventional supine MRIs who also reported pain during epidural distension in the prone position or who reported similar pain while lying in the prone position.

The aim of our study is to comparatively evaluate prone vs supine MRIs in patients with moderate-to-severe LBP and/or radicular pain whose conventional MRI was reported as negative and who were nonresponsive to treatment.

METHODS

This prospective study was performed in compliance with the hospital ethical committee requirements following approval from the Hospital Group Madrid Clinical Research Ethics Committee (Code: 17.01.1040-GHM). All patients received verbal information about the study and written informed consent was obtained in all cases.

Nineteen patients suffering chronic moderate-to-severe LBP with or without accompanying radicular pain (Numeric Rating Scale [NRS-11] > 4), nonresponsive to conventional treatments, such as multimodal analgesia, physical therapy, and interventional treatments (e.g., epidural blocks, facet blocks, pulsed radio-frequency), were included in the study.

Inclusion criteria were moderate-to-severe chronic LBP, anodyne supine MRI, normal dynamic X-ray study, poor response to treatments, and pain worsening during epidural distension and in the prone position. Exclusion criteria included pregnancy, age < 18 years, and contraindication for MRI due to the presence of ferromagnetic material in the body.

Clinical and demographic data were collected, and supine and prone MRI measurements obtained. These included spinal canal area, lateral recess diameter, foraminal area, and ligamentum flavum thickness.

The MRI study protocol was similar in all cases. This

included a 1.5 T MRI apparatus (Siemens Espree, Berlin, Germany), equipped with multichannel spine antennas (i.e., adding multichannel body antennae in prone studies). Patients were studied in supine and prone positions.

The patients were positioned with their legs extended in both phases of the study in order not to vary the alignment of the spine due to leg flexion or extension.

Study in Supine Position

For the sagittal T2 turbo spin echo (TSE), the following settings were used: repetition time (TR) 2,000 milliseconds, echo time (TE) 140 milliseconds, slice thickness of 4 mm, gap of 0.4 mm. Field of view (FOV) of 28 cm and 256 x 256 matrix.

For the axial T2 TSE, 5 slices were obtained for each lumbar segment analyzed, with TRs 2000-300 milliseconds, TE 120 milliseconds, FOV 25 cm, matrix 256 x 224, and slice thickness of 4 mm and gap of 0.5 mm.

The settings used for sagittal T1 were a TR of 350-400 milliseconds, TE 25 milliseconds, slice thickness 4 mm, FOV 44 cm, and matrix 512 x 256.

Study in Prone Position

Sagittal T2 TSE and axial T2 TSE were executed using same protocol as for the supine position. Because the nomenclature of disc pathology may be confusing (10), we have employed the most commonly used definitions (11):

- Disc bulging: circumferential enlargement of the disc, symmetrical or asymmetrical.
- Disc herniation: disc protrusion or extrusion from a focal bulge, generally ≥ 3 mm, outside the vertebral margin.
- Disc protrusion: eccentric herniation with a wide-base connection with the disc, such that, in any plane, the greatest possible distance between the margins of the disc material protruding from the margin of the disc space is less than the distance between the margins of the base considered in the same plane.
- Disc extrusion: eccentric focal bulge that retains a thin pedicle connecting to the disc.

The different parameters that were measured were defined as follows (Fig. 1) (11,12):

- a- Spinal canal area (measured in mm²): Sectional area of the canal in axial slices at the level where the disc has maximum expressivity. In general, it

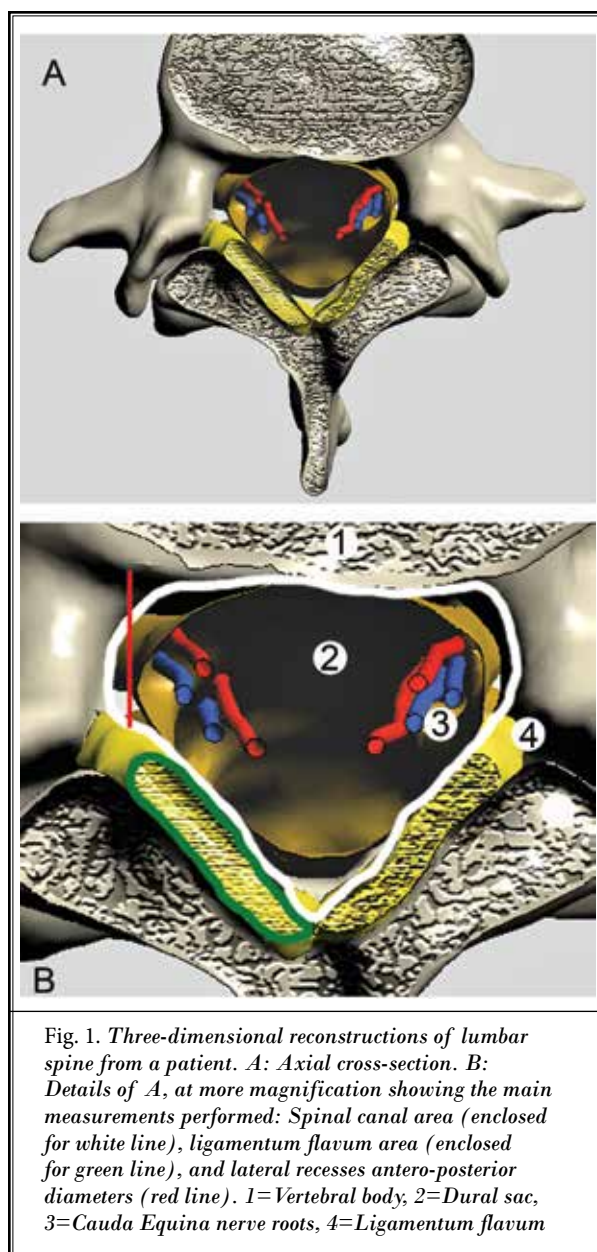


Fig. 1. Three-dimensional reconstructions of lumbar spine from a patient. A: Axial cross-section. B: Details of A, at more magnification showing the main measurements performed: Spinal canal area (enclosed for white line), ligamentum flavum area (enclosed for green line), and lateral recesses antero-posterior diameters (red line). 1=Vertebral body, 2=Dural sac, 3=Cauda Equina nerve roots, 4=Ligamentum flavum

corresponds to an area of triangular morphology, whose anterior margin is determined by the disc contour (covered, if it is the case, by the posterior vertebral ligament, from which it is not differentiated), the anterior vertices are located at the level of the lateral recesses and the posterior vertice of the triangle is located at the posterior midline in the confluence of the flavum ligaments. It includes the thecal sac with its roots and the epidural recesses.

- b- Ligamentum flavum area: Due to the low signal of

these structures, it is sometimes difficult to determine their limit with respect to the bony cortex of the internal faces of the laminae, being extremely cautious when it was necessary to consider them equally in both positions.

- c- Lateral recesses diameters: In axial sections, antero-posterior diameters of both lateral recesses, right and left, corresponding to the distances between the disc margin covered by the posterior vertebral ligament (anterior limit) and the cranial part of the articular facet covered by the ligamentum flavum.
- d- Intervertebral foramina area: Both right and left foramina in each segment on sagittal slices. Ideally, zone II of Anderson and McNeill (12), at pedicle level, has been considered, whenever possible, as upper and lower limits.

In case of disc herniation, a quantitative analysis was also performed, and measurements were taken at the level of greatest asymmetric protrusion.

All measurements from MRI were made by a neuroradiologist.

Three-dimensional (3D) reconstruction of the different patterns of pathology were made. The different pathologies were shown using the 3D-portable document format (PDF) model available for download at <http://diposit.ub.edu/dspace/handle/2445/44844?locale=en>

Images were captured from this model and modified using Photoshop (Adobe, San Jose, CA, United States) to simulate these pathologies and better understand our acquired images.

The research team previously performed interactive 3D reconstructions of the lumbar spine MRIs from the second lumbar vertebra to the sacrum of 7 patients with normal MRIs (13). In short, we used Philips Intera 1.5 team software (Philips Intera 1.5 team software, 1.1 Tesla, Amsterdam, The Netherlands). For the 3D reconstruction, we selected 2 sequences, namely the Fast Field Echo 3D T1 sequence and the T2 Balance sequence. To achieve optimal image reconstruction, weighted sequences in T1 and T2 (axial plane) were obtained with an isometric voxel configuration and an overlap of about 50% of the acquired data. Voxels x, y, and z equal to 0.6 mm were selected to create models from the high-resolution images. The technical MRI details and the method for obtaining the 3D PDF model of lumbar structures have been described elsewhere (13,14). The 3D PDF format was used to facilitate analysis of the images without the need for any additional sophisticated software. Briefly, axial sequence MRI acquisitions were

grouped into 2 aligned, adjacent blocks of 130 mm each, that is, a caudal and a rostral MRI block extending from the lowest end of the dural sac to the lower thoracic vertebrae (T11 or T10). The number of acquisitions depended on patient height. MRIs were acquired at 16 bits and exported in Digital Imaging and Communication in Medicine format. Files were analyzed using Amira version 5.2 3D software (Mercury Co., Boston, MA) installed on a Dell Precision graphic station.

The T2-weighted sequence was used for cerebrospinal fluid and nerve root volume estimations. The T1 fast-field echo sequence allowed 3D reconstruction of the dural sac and surrounding structures: ligamentum flavum, vertebrae, intervertebral discs, and ligaments. We performed manual delimitation of the volume of interest of the 3D-reconstructed structures, surface generation by triangulation of volumes of interest (0.01 cm² per triangle), automatic smoothing of the model, and revision of the correspondence between each model's contours and its corresponding structure in the MRIs. Models and MRI planes were exported to Virtual Reality Modeling Language file format. Virtual Reality Modeling Language files were imported to 3D Reviewer (Tetra 4D, Seattle, WA) to generate a universal 3D file format, which contained graphical components that were compatible with PDF documents. Acrobat XI Pro (Adobe, Adobe Inc., San Jose, CA) was used to define a title area (superior), JavaScript-controlled buttons (left), and links to predefined scenes of interest (below). The accessory plug-in "3D PDF converter" (Tetra 4D, Bend, OR) allowed us to embed the universal 3D files into a 3D control area.

Statistical Analysis

Data are presented as media + standard deviation or media and range when appropriate. Global MRI measurements between supine/prone positions were compared using a Wilcoxon signed-rank test. Significance was set at $P < 0.05$.

RESULTS

Twenty-one patients were initially included in the study. In 2 cases, MRI was contraindicated and these patients were excluded. The mean age was 48.7 years (range [R]: 30-69), 63% women, with a mean numeric pain score (NRS-11) of 6.5 (R: 4-8). Clinical and demographic data and main findings in both supine and prone MRI studies are shown in Table 1.

In the prone position, 6 cases of 19 were found to have herniated discs that could not be assessed in the

Prone Position MRI of the Lumbar Spine

Table 1. Clinical and demographic data. Main findings in both supine and prone MRI studies.

Patient No, Gender	Age (y)	NRS-11	Symptoms	Supine MRI	Prone MRI
M	30	6	Bilateral LBP + Right Radiculopathy	Normal	L4-L5 Disc Prolapse, Buckling, and Increase Thickness of the Ligamentum Flavum
W	63	7	Left-Side LBP	Normal	L4-L5 Left Paramedial Hernia, Ligamentum Flavum Buckling
M	32	8	Bilateral LBP	L4-S1 Posterior Arthrodesis	L3-L4 Listhesis + Disc Herniation
M	52	7	Right-Side LBP	L5-S1 Right Laminectomy	Ligamentum Flavum Buckling
M	40	5	Bilateral LBP	Facet Osteoarthritis	Ligamentum Flavum Buckling
W	37	8	Bilateral LBP + Left Radiculopathy	L4-L5 Posterior Arthrodesis	L4-L5 /L5-S1 Disc Herniations
W	56	5	Bilateral LBP + Radiculopathy	L4-L5 Disc Bulging	L4-L5 Listhesis + Disc Herniation
W	63	7	Bilateral LBP + Radiculopathy	L2-L3/L3-L4 Disc Protrusions	L2-L3/L3-L4 Disc Herniations, Ligamentum Flavum Buckling, Stenosis
W	60	7	Left-Side LBP + Radiculopathy	L4-L5 Disc Protrusion	L4-L5 Disc Herniation, Lateral Stenosis
W	48	6	Right-Side LBP + Radiculopathy	L4-L5 Disc Bulging	Increased Right L4-L5 Disc Protrusion
W	46	8	LBP + Right Radiculopathy	L4-L5/L5-S1 Disc Bulging	Severe L5-S1 Lateral Stenosis, Facet Joint Subluxation
W	56	5	Bilateral LBP	L3-L4 Disc Bulging	Decreased Foraminal Area L3-L4/L4-L5, Increased L3-L4 Disc Protrusion
W	44	4	Bilateral LBP	Normal	Decreased Foraminal Area L4-L5/L5-S1, Lateral Stenosis
M	43	7	Right Radiculopathy	Normal	Decreased Right L3-L4/L4-L5 Foraminal Area, Increased Right Side Ligamentum Flavum Thickness
W	54	5	Bilateral LBP	L4-L5 Right Laminectomy	Ligamentum Flavum Buckling
W	69	7	Left LBP	L3-L4/L4-L5/L5-S1 Disc Bulging	L5-S1 Ligamentum Flavum Buckling, Decreased Left L5-S1 Foraminal Area, Lateral Stenosis
W	44	6	Bilateral LBP + Radiculopathy	L4-L5/L5-S1 Disc Protrusions	Ligamentum Flavum Buckling
W	38	8	Right Radiculopathy	L4-L5 Protrusion	Decreased Right L4-L5 Foraminal Area, Severe L4-L5 Right Lateral Stenosis
M	50	8	Bilateral LBP	L5-S1 Disc Bulging	L5-S1 Disc Protrusion, Decreased Foraminal Area L4-L5/L5-S1, Ligamentum Flavum Buckling

Abbreviations: MRI, magnetic resonance imaging; NRS-11, numeric rating scale; M, man; W, woman; LBP, low back pain.

supine position (Fig. 2), and in 4 cases, prolapsed discs not seen in the supine MRI were found. Measurements obtained in supine vs prone MRI studies are reported in Table 2.

On prone images, we identified significant buckling and increased ligamentum flavum thickness in 10 of the 19 patients (52.6 %) (Fig. 3) that we did not observe on the supine MRIs. Five patients (26.3%) had newly discovered degrees of spondylolisthesis (Fig. 4) and facet joint subluxation that resulted in significant foraminal stenosis in the prone position (Fig. 5).

Figures 6 through 9 show 3D reconstructions of the MRI images of the main findings described in this study.

DISCUSSION

This study of prone MRI in patients with no MRI evidence of pathology on supine MRI and poor response to conservative therapies revealed at least 4 patterns of findings that permit better explanation of their clinical outcomes. These include: (i) occurrence of disc herniations or protrusions, (ii) thickening, buckling, or folding of the ligamentum flavum, (iii) spondylolisthesis, and

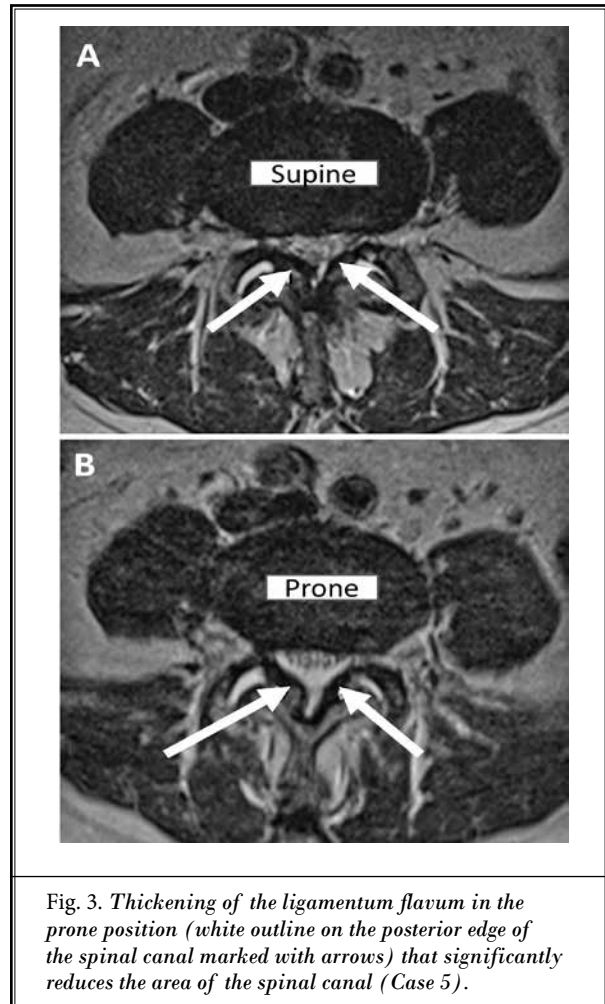
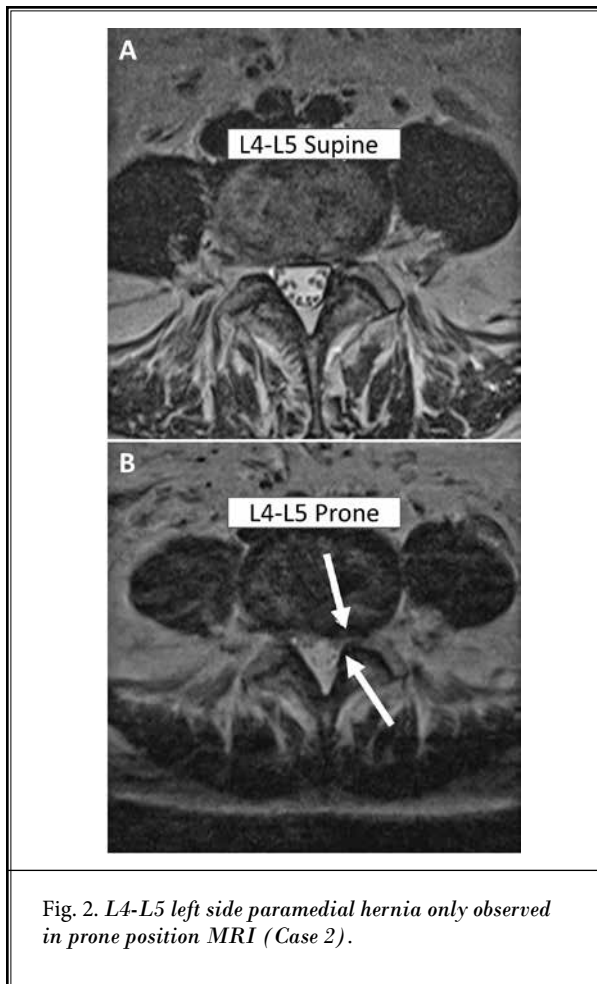


Table 2. Measurements obtained in supine vs prone MRI studies ($n = 19$, mean \pm SEM).

	Supine	Prone	P value
Spinal Canal Area (mm ²)	255.60 \pm 14.26	230.42 \pm 15.10	$P < 0.001$
Foraminal Area (mm ²)	195.26 \pm 15.24	156.60 \pm 15.29	$P < 0.005$
Ligamentum Flavum Thickness (mm ²)	107.87 \pm 7.05	125.47 \pm 10.10	$P < 0.005$
Lateral Recess Diameter (mm)	6.25 \pm 0.47	5.27 \pm 0.60	N.S.

Abbreviation: MRI, magnetic resonance imaging; SEM, standard error of mean; N.S., not significant.

(iv) foraminal stenosis. These results seem to indicate a certain degree of segmental instability, mainly linked to the soft tissue/non-bony elements of the spinal canal.

Segmental instability has to date been studied by

functional flexion and extension radiographs of the spine in the standing position. However, with this test, the involvement of soft tissues, such as the ligamentum flavum, disc material, or facet joint capsules, cannot be evaluated. In the current study, all patients had normal dynamic radiological studies. Dynamic MRI studies (2,3) have provided some insight into the involvement of other non-bony soft tissue structures, and this extended the concept of segmental dynamic instability to the soft tissues and posterior vertebral joints.

CT and MRI studies performed under the axial load technique with a compression force applied to the patient by different devices have also been tested, but it does not seem clear that they can reproduce sufficient physiological loading conditions to detect instability (15).

While dynamic upright MRI of the spine has been performed for many years, and it is known that it increases the sensitivity for the detection of disc pathol-

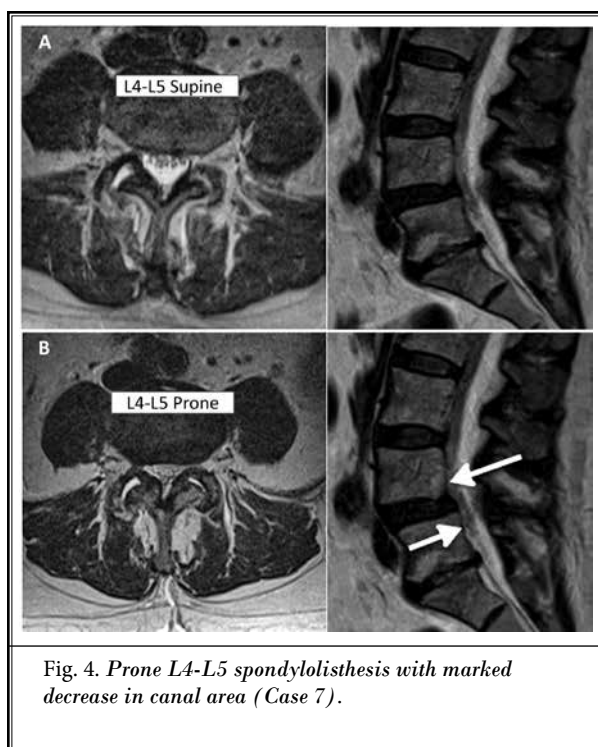


Fig. 4. Prone L4-L5 spondylolisthesis with marked decrease in canal area (Case 7).

ogy and canal stenosis undetected with conventional MRI, it is not clear if they contribute anything to the specificity of the diagnosis (16). In fact, one of the major criticisms of these studies has been that they may reveal findings unrelated to the real pain-generating mechanisms (9) as they often reveal false-positive findings that could lead to unnecessary surgery or other treatments. To the best of our knowledge, this is the only clinical study that correlates MRI findings with patients' symptomatology otherwise unexplainable with conventional MRI, thus minimizing both the false-negative rate of conventional MRI and the false-positive rate of dynamic studies performed without clinical correlation.

The findings of the standing MRI studies (2-4) are essentially the same as those obtained in our work with prone position MRI. Prone MRI could thus be a good and technically easier substitute for standing MRI. Its advantages would be (i) both supine and prone studies can be performed in the same machine, (ii) higher image quality (prone MRIs usually do not exceed 0.25 T), (iii) it allows immediate comparison of the same segments to be studied, and (iv) it is more accessible to the general population and most hospital centers could perform it.

The findings of this study have treatment implications. The high incidence of dynamic disc pathology

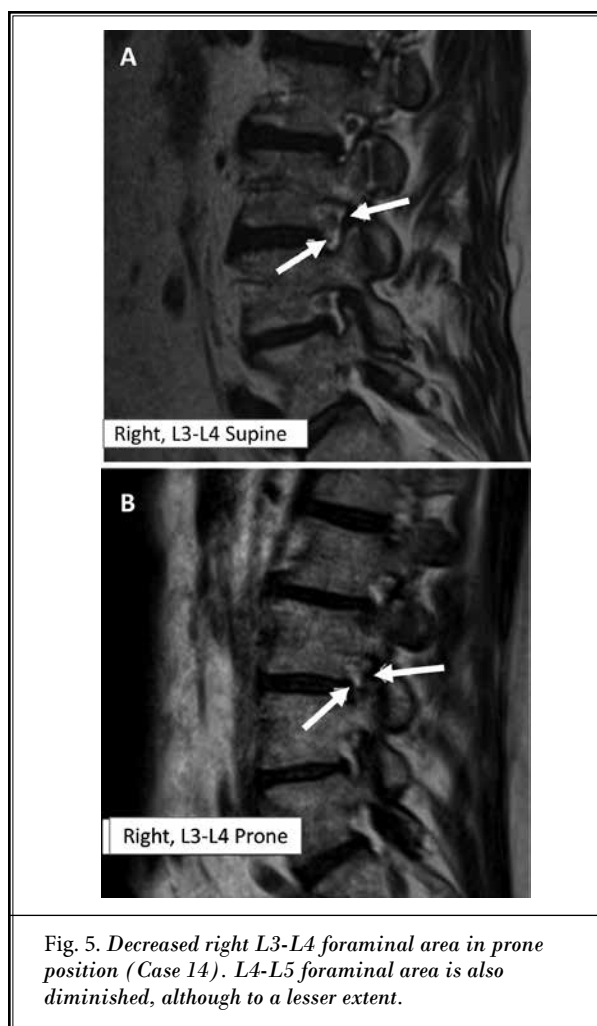


Fig. 5. Decreased right L3-L4 foraminal area in prone position (Case 14). L4-L5 foraminal area is also diminished, although to a lesser extent.

that is only observed, or exacerbated, in the prone position seems to recommend the use of the different techniques of nucleoplasty, nucleotomy, or minimally invasive percutaneous discectomy for its treatment (17). In this sense, more prospective studies are needed.

However, to our knowledge, the most striking finding is the high incidence of thickening, folding, or buckling of the ligamentum flavum, observed in almost half of the patients. This may contribute to both global canal and recess symptomatic stenosis. Conservative flavectomy techniques, such as percutaneous or interventional endoscopy spinal surgery, which are not commonly used, could be considered in these selected patients (18).

The limitations of this study include the lack of a control group and the small sample size. More extensive works will be necessary to further develop the conclusions of this study.

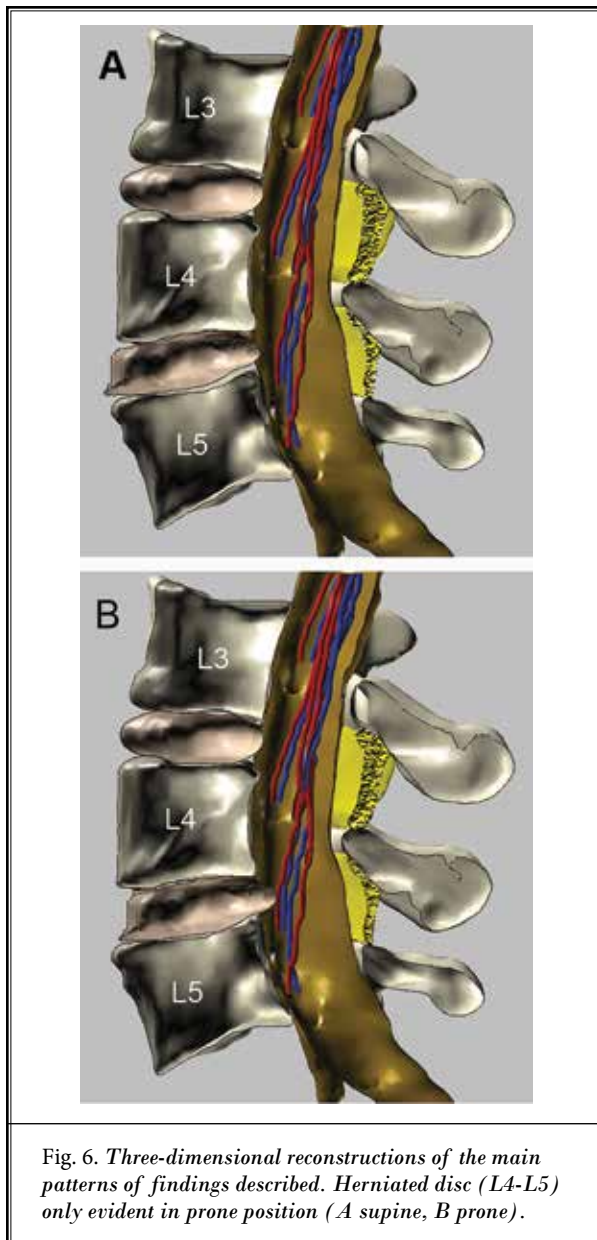


Fig. 6. Three-dimensional reconstructions of the main patterns of findings described. Herniated disc (L4-L5) only evident in prone position (A supine, B prone).

CONCLUSIONS

Prone MRI of the lumbar spine in patients with LBP, with or without radicular pain not clarified with conventional MRI, can shed light on the origin of the patient's pain. It can also help to decide the most appropriate treatment for each case. Larger studies are

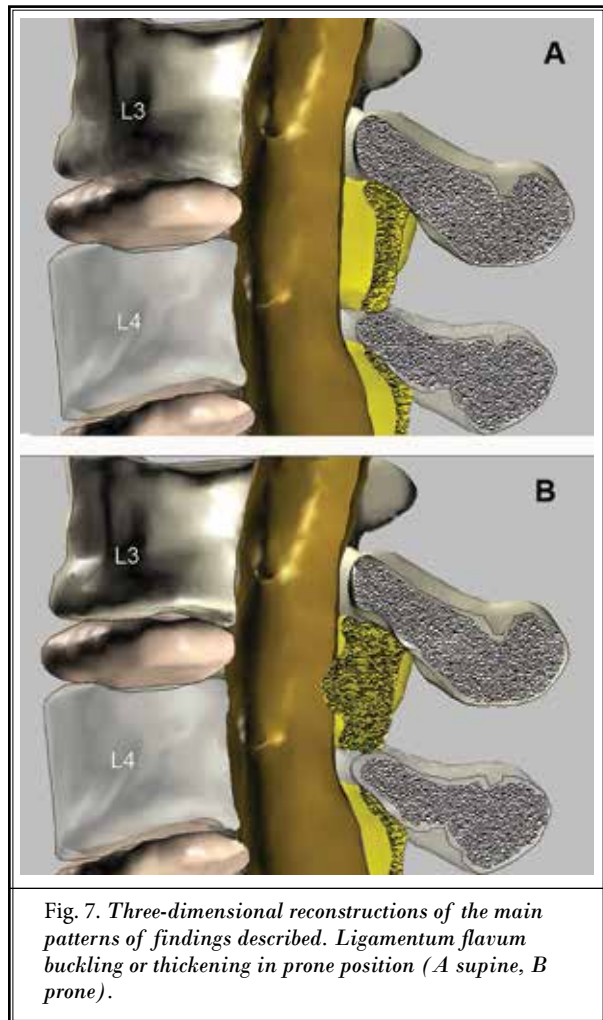


Fig. 7. Three-dimensional reconstructions of the main patterns of findings described. Ligamentum flavum buckling or thickening in prone position (A supine, B prone).

needed to establish its definitive role in the management of the patient with LBP.

Acknowledgments

The authors sincerely thank Corey Astrom, ELS, and Leah Buletti of the University of Florida, Gainesville, Florida, United States for their help with the preparation of this manuscript. They would also like to thank Laura Barrigón for the review of the statistical analysis.

Ethics Approval

Hospital Group Madrid Clinical Research Ethics Committee (Code: 17.01.1040-GHM).

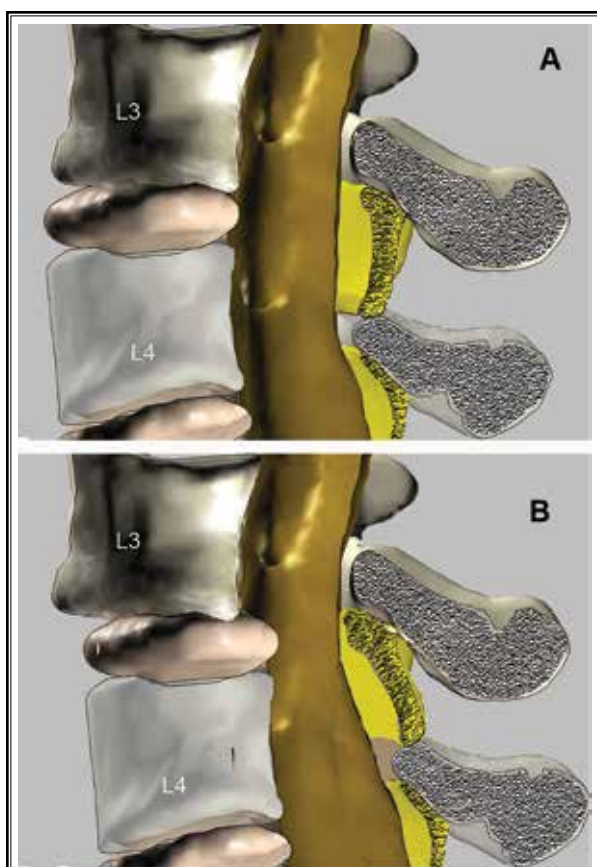


Fig. 8. Three-dimensional reconstructions of the main patterns of findings described. Spondylolisthesis (L3-L4) in prone position (A supine, B prone).

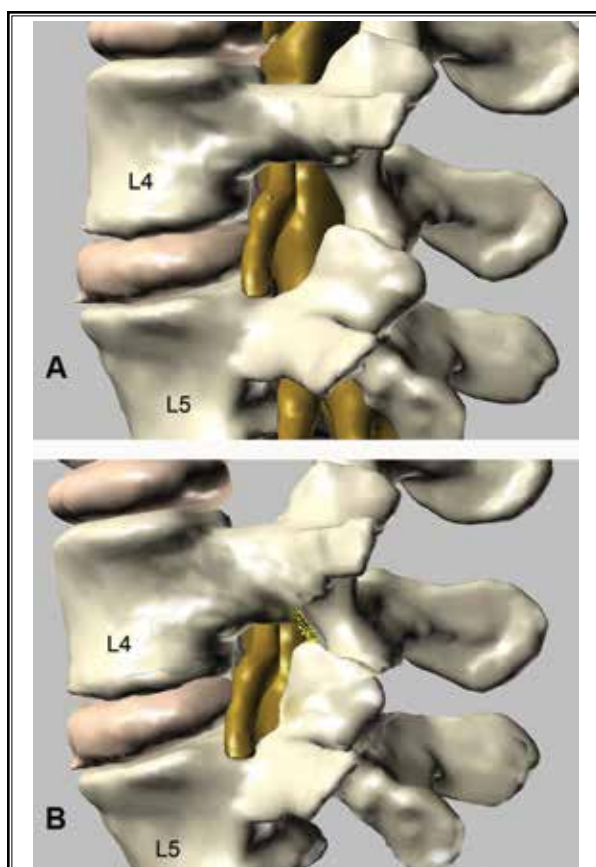


Fig. 9. Three-dimensional reconstructions of the main patterns of findings described. Narrowing of the intervertebral foramen in prone position (A supine, B prone).

REFERENCES

1. D'Andrea G, Ferrante L, Dinia L, Caroli E, Orlando ER. "Supine-Prone" dynamic x-ray examination new method to evaluate low-grade lumbar spondylolisthesis. *J Spinal Disord Tech* 2005; 18:80-83.
2. Hansen BB, Nordberg CL, Hansen P, et al. Weight-Bearing MRI of the lumbar spine: Spinal stenosis and spondylolisthesis. *Semin Musculoskelet Radiol* 2019; 23:621-633.
3. Michelini G, Corridore A, Torlone S, et al. Dynamic MRI in the evaluation of the spine: State of the art. *Acta Biomed* 2018; 89:89-101.
4. Berry DB, Hernandez A, Onodera K, Ingram N, Ward SR, Gombatto SP. Lumbar spine angles and intervertebral disc characteristics with end-range positions in three planes of motion in healthy people using upright MRI. *J Biomech* 2019; 89:95-104.
5. Nakanishi K, Tanaka N, Kamei N, et al. Use of prone position magnetic resonance imaging for detecting the terminal filum in patients with occult tethered cord syndrome. *J Neurosurg: Spine* 2013; 18:76-84.
6. Tsuchida R, Sumitani N, Azuma K, et al. A novel technique using magnetic resonance imaging in the supine and prone positions for diagnosing lumbar adhesive arachnoiditis: A preliminary study. *Pain Practice* 2020; 20:34-43.
7. Vaccaro AR, Kepler CK, Rihn JA, et al. Anatomical relationships of the anterior blood vessels to the lower lumbar intervertebral discs analysis based on magnetic resonance imaging of patients in the prone position. *J Bone Joint Surg Am* 2012; 94:1088-1094.
8. Cecen GS, Gulabi D, Cecen A, Oltulu I, Guclu B. Computerized tomography imaging in adolescent idiopathic scoliosis: Prone versus supine. *Eur Spine J* 2016; 25:467-475.
9. Hansen BB, Hansen P, Grindsted J, et al. Conventional supine MRI with a lumbar pillow—an alternative to weight-bearing MRI for diagnosing spinal stenosis? A cross-sectional study. *Spine* 2017; 44:662-669.
10. Arana E, Royuela A, Kovacs FM, et al. Lumbar spine: Agreement in the interpretation of 1.5-T MR images by using the Nordic Modic Consensus Group classification form. *Radiology* 2010; 254:809-817.
11. Fardon DF, Williams AL, Dohring EJ, Murtagh FR, Rothman SLG, Sze GK.

- Lumbar disc nomenclature: Version 2.0: Recommendations of the combined task forces of the North American Spine Society, the American Society of Spine Radiology, and the American Society of Neuroradiology. *Spine (Phila Pa 1976)* 2014; 39:E1448-E1465.
12. Anderson, GBJ, McNeill TW (eds). *Lumbar Spine Syndromes*, Springer Verlag, Vienna, Austria, 1989.
 13. Prats-Galino A, Reina MA, Mavar M, Puigdellívol-Sánchez A, San-Molina J, De Andrés JA. 3D interactive model of lumbar spinal structures of anesthetic interest. *Clin Anat* 2015; 28:205-212.
 14. Reina MA, Lirk P, Puigdellívol-Sánchez A, Mavar M, Prats-Galino A. Ligamentum flavum anatomy for epidural anesthesia: Reviewing a 3D MR-based interactive model and postmortem samples. *Anesth Analg* 2016; 122:903-907.
 15. Manenti G, Liccardo G, Sergiacomi G, et al. Axial loading MRI of the lumbar spine. *In Vivo* 2003; 17:413-420.
 16. Hansen BB, Hansen P, Carrino JA, Fournier G, Rasti Z, Boesen M. Imaging in mechanical back pain: Anything new?. *Best Pract Res Clin Rheumatol* 2016; 30:766-785.
 17. Ong D, Chua NH, Vissers K. Percutaneous disc decompression for lumbar radicular pain: A review article. *Pain Pract* 2016; 16:111-126.
 18. Lee CW, Yoon KJ, Jun JH. Percutaneous endoscopic laminectomy with flavectomy by uniportal, unilateral approach for the lumbar canal or lateral recess stenosis. *World Neurosurg* 2018; 113:e129-e137.